Plasmonic Waveguide Analysis

Sergei Yushanov, Jeffrey S. Crompton*, and Kyle C. Koppenhoefer

AltaSim Technologies, LLC

*Corresponding author: 130 E. Wilson Bridge Road, Suite 140, Columbus, OH 43085, jeff@altasimtechnologies.com

Abstract:

This paper compares numerical and analytic solutions for a typical plasmonic waveguide consisting of a thin film sandwiched between a cladding cover and a substrate. Two configurations are analyzed using the Electromagnetic Waves, Frequency Domain interface (emw) of the RF Module of COMSOL Multiphysics: dielectric-metal dielectric (DMD) and metal-dielectric-metal (MDM) layers. The analytic solution developed by Orfanidis [1] provides a comparison with the numerical results.

Keywords: Plasmonic waveguide, electromagnetics, analytic solution.

1. Introduction

Surface Plasmons (SP) or Surface Plasmon Polaritons (SPP) are electromagnetic excitations that propagate at the interface between a dielectric and a conductor, and are evanescently confined in the perpendicular direction to the propagation. They arise via coupling of the electromagnetic field to oscillations of the conductor's electron plasma and are characterized in terms of dispersion and spatial profile. From an electrodynamic view, SPs are a particular case of a surface wave: from the optics view, SPs are optical modes of an interface: from the solid-state physics view, SPs are collective excitation of electrons. The behavior of Surface Plasmons can be described by Maxwell's equations as long as the properties of metals at optical frequencies can be obtained from experiment or theoretically calculated from the Drude model of electron conduction.

Surface plasmonic waveguides have the ability to confine light at sub-wavelength scale and have a large number of applications in the field of nanocircuits, nanophotonics devices, biological and chemical sensors, holography, and other applications. Use of plasmons in electric circuits, or in an electric circuit analog, combines the size efficiency of electronics with the data capacity of photonic integrated circuits. Both surface plasmon polaritons propagating along the metal-dielectric interfaces and localized surface plasmon modes supported by metal nanoparticles are characterized by large momentum values, which enable strong resonant enhancement of the local density of photon states and can be utilized to enhance weak optical effects of opto-electronic devices. Different plasmonic waveguide structures have been proposed, such as layered structures, metallic nanowires, metallic nanoparticle arrays, hybrid wedge plasmonic waveguides, and other configurations. Here, a typical plasmonic waveguide consisting of a thin film sandwiched between a cladding cover and a substrate will be considered. Two configurations are analyzed using the Electromagnetic Waves, Frequency Domain interface (emw) of the RF Module of COMSOL Multiphysics: dielectric-metal dielectric (DMD) and metal-dielectric-metal (MDM) layers. Results are compared against an analytic solution developed by Orfanidis [1].

2. Double Interface Plasmonic Waveguide – Analytic Solution

The waveguide geometry for the DMD and MDM configurations is shown in Fig. 1. The waveguide consists of a thin film ε_f, sandwiched between a cladding cover ε_c and a substrate ε_s. The layers have infinite extent along the $z-$ direction. In the DMD configuration, the film layer is metal, while substrate and cladding are dielectric layers. In the MDM configuration, the film layer is dielectric, and metals are substrate and cladding. Only TM plasmonic modes will be considered, although TE modes are also possible in more

complicated media, such as metamaterials and magnetic materials [2].

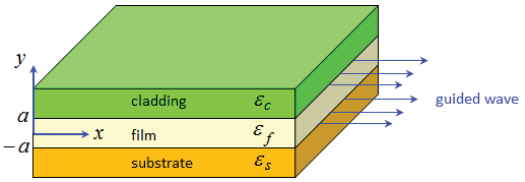

Figure 1. Plasmonic waveguide in either DMD of MDM configuration.

The analytical solution given below is taken from textbook by Orfanidis [2]. In a waveguiding system shown in Fig. 1, the electric and magnetic fields are propagating along the guiding x direction. The layers have infinite extent along the $z-$direction. Fields are assumed to have the following form:

$$\mathbf{E}(x,y,t)=\mathbf{E}(y)e^{j\omega t-j\beta x}$$
$$\mathbf{H}(x,y,t)=\mathbf{H}(y)e^{j\omega t-j\beta x} \quad (1)$$

where β is the propagation wavenumber along the guide $x-$direction.

For TM modes, there is one longitudinal field E_x and two transverse fields E_y, H_z. The rest components of the electromagnetic wave are zero. The longitudinal field satisfies the Helmholtz equation

$$\frac{\partial^2 E_x}{\partial y^2}-k_c^2 E_x=0 \quad (2)$$

The transverse electric field E_y is computed from Maxwell's equations in terms of longitudinal field:

$$E_y=-\frac{j\beta}{-k_c^2}\frac{\partial E_x}{\partial y} \quad (3)$$

The transverse magnetic field H_z is obtained from transverse electric field and TM impedance

$$\eta_{TM}:\ H_z=\frac{1}{\eta_{TM}}E_y,\quad \eta_{TM}=\frac{\beta}{\omega\varepsilon_0\varepsilon} \quad (4)$$

The cutoff wavenumber k_c appearing in the Helmholtz equation depends on dielectric constant ε of the propagating medium, $k_c^2=k_0^2\varepsilon-\beta^2$, where $k_0=2\pi/\lambda_0=\omega/c_0$ is the vacuum wavenumber and λ_0 is the vacuum wavelength, and c_0 is free-space speed of light. Therefore, k_c takes different values in each layer.

Within the film with a dielectric constant of ε_f, the transverse cutoff wavenumber satisfies $k_{cf}^2=k_0^2\varepsilon_f-\beta^2$. The fields cannot penetrate into the metal and will be essentially surface wave that decay exponentially away from the metal dielectric interface. Defining film attenuation coefficient by $\gamma=jk_{cf}$, we obtain the following relationship within the film region:

$$\gamma^2=\beta^2-k_0^2\varepsilon_f,\quad |y|\le a \quad (5)$$

We look for field solutions that decay exponentially away from interfaces so that cutoff wavenumbers in substrate and cladding regions are pure imaginary. Defining transverse attenuation coefficients by $\alpha_c=jk_{cc}$ for cladding and $\alpha_s=jk_{cs}$ for substrate, we obtain the following relations:

$$\alpha_c^2=\beta^2-k_0^2\varepsilon_c,\quad y\ge a$$
$$\alpha_s^2=\beta^2-k_0^2\varepsilon_s,\quad y\le -a \quad (6)$$

Thus, the TM modes are obtained by solving the Helmholtz equation in each layer

$$\begin{cases}\dfrac{\partial^2 E_x}{\partial y^2}-\gamma^2 E_x=0, & \text{for } |y|\le a\\ \dfrac{\partial^2 E_x}{\partial y^2}-\alpha_c^2 E_x=0, & \text{for } y\ge a\\ \dfrac{\partial^2 E_x}{\partial y^2}-\alpha_s^2 E_x=0, & \text{for } y\le -a\end{cases} \quad (7)$$

Equation (7) is supplemented by the continuity boundary conditions for the tangential fields at the layer interfaces:

$$E_x\big|_{y=-a-0} = E_x\big|_{y=-a+0}, \quad E_x\big|_{y=a-0} = E_x\big|_{y=a+0} \tag{8}$$

$$\begin{aligned} H_z\big|_{y=-a-0} &= H_z\big|_{y=-a+0} \\ H_z\big|_{y=a-0} &= H_z\big|_{y=a+0} \end{aligned} \tag{9}$$

Inside the film, the solution to the Helmholtz equation can be constructed using linear combination of hyperbolic terms $\sinh(\gamma y)$ and $\cos(\gamma y)$ - referred to as *plasmonic solutions*. The solution that automatically satisfies the continuity boundary conditions (8) can be expressed as following:

$$E_x(y) = \begin{cases} E_0 \sinh(\gamma y + \psi), & |y| \le a \\ E_0 \sinh(\gamma a + \psi) e^{-\alpha_c (y-a)}, & y \ge a \\ E_0 \sinh(\gamma a - \psi) e^{\alpha_s (y+a)}, & y \le -a \end{cases} \tag{10}$$

Transverse electric field is obtained from relation (3):

$$E_y(y) = \begin{cases} -\frac{j\beta}{-\gamma^2}\frac{\partial E_y}{\partial x} = E_0 \frac{j\beta}{\gamma}\cosh(\gamma y + \psi), & |y| \le a \\ -\frac{j\beta}{-\alpha_c^2}\frac{\partial E_y}{\partial x} = -E_0 \frac{j\beta}{\alpha_c}\sinh(\gamma a + \psi) e^{-\alpha_c (y-a)}, & y \ge a \\ -\frac{j\beta}{-\alpha_s^2}\frac{\partial E_y}{\partial x} = E_0 \frac{j\beta}{\alpha_s}\sinh(\gamma a - \psi) e^{\alpha_s (y+a)}, & y \le -a \end{cases} \tag{11}$$

The transverse magnetic field is then obtained from the relation (4), where TM impedance is defined as $\eta_{TM} = \beta / \omega\varepsilon_0\varepsilon_f$ for film layer, $\eta_{TM} = \beta / \omega\varepsilon_0\varepsilon_c$ for cladding layer, and $\eta_{TM} = \beta / \omega\varepsilon_0\varepsilon_s$ for substrate.

The interface continuity conditions of the tangential H-field (9) yield the following two equations:

$$\begin{aligned} \tanh(\gamma a + \psi) &= -\frac{\varepsilon_f \alpha_c}{\varepsilon_c \gamma} \\ \tanh(\gamma a - \psi) &= -\frac{\varepsilon_f \alpha_s}{\varepsilon_s \gamma} \end{aligned} \tag{12}$$

Five parameters β, γ, α_c, α_s, ψ are determined from five transcendental algebraic equations (5), (6), (12).

The field amplitude E_0 can be obtained from total power P_0 transmitted in plasmonic waveguide. The $x-$component of the Poynting vector gives the power flow in the $x-$direction per unit area:

$$\begin{aligned} \mathcal{P}_x &= \frac{1}{2}\mathrm{Re}\left[E_y(y) H_z^*(y)\right] = \\ &\frac{1}{2}\mathrm{Re}\left[1/\eta_{TM}\right] \left|E_y(y)\right|^2 \end{aligned} \tag{13}$$

Integrating (13) over the area yz, we obtain the net power transmitted along the $x-$direction:

$$\begin{aligned} P_0 &= \left(\int_{-\infty}^{-a} \mathcal{P}_x dy + \int_{-a}^{a} \mathcal{P}_x dy + \int_{a}^{\infty} \mathcal{P}_x dy\right) w = \\ &P_s + P_f + P_c \end{aligned} \tag{14}$$

where w is dimension of waveguide in the $z-$direction. Power transmitted in the substrate, film layer, and cladding is obtained as

$$\begin{aligned} P_s &= \xi\,\mathrm{Re}\left[\frac{\beta}{k_0\varepsilon_s}\right]\frac{\left|\cosh(\gamma a - \psi)\right|^2}{2\,\mathrm{Re}[\alpha_s]} \\ P_f &= \xi\,\mathrm{Re}\left[\frac{\beta}{k_0\varepsilon_f}\right]\left\{\frac{\sinh(2\,\mathrm{Re}[\gamma]a)\cosh(2\,\mathrm{Re}[\psi])}{2\,\mathrm{Re}[\gamma]} + \frac{\sin(2\,\mathrm{Im}[\gamma]a)\cos(2\,\mathrm{Im}[\psi])}{2\,\mathrm{Im}[\gamma]}\right\} \\ P_c &= \xi\,\mathrm{Re}\left[\frac{\beta}{k_0\varepsilon_c}\right]\frac{\left|\cosh(\gamma a - \psi)\right|^2}{2\,\mathrm{Re}[\alpha_c]} \end{aligned} \tag{15}$$

where $\xi = \frac{1}{2} w \eta_0 \left|H_0\right|^2$,

$H_0 = j\omega\varepsilon_0\varepsilon_f E_0 / \gamma$, and $\eta_0 = \sqrt{\mu_0 / \varepsilon_0}$.

3. Use of COMSOL Multiphysics

Geometry of the 2D model is shown in Fig. 2, where film is sandwiched between a substrate and a cladding cover. TM polarized wave is guided in the $x-$direction. Thickness of the film is $1\mu m$. Plasmonic waveguides are operated at optical or infrared frequencies where the metal has permittivity with negative real part. Dielectric constants of the layers are given in Table 1.

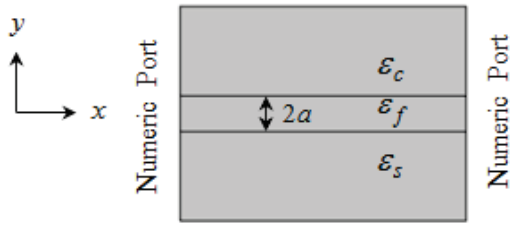

Figure 2. Comsol model of plasmonic waveguide.

Table 1. Dielectric constants of the layers.

Configuration	Substrate, ε_s	Film, ε_f	Cladding, ε_c
DMD	1.7	-4	3.5
MDM	-1.6	2.2	-4

Electromagnetic wave propagation is governed by Maxwell's wave equation in frequency domain:

$$\nabla\times\frac{1}{\mu_r}(\nabla\times\mathbf{E})-k_0^2\left(\varepsilon_r-\frac{j\sigma}{\omega\varepsilon_0}\right)\mathbf{E}=0 \qquad (16)$$

Electromagnetic Waves, Frequency Domain (emw) physics interface is used to solve governing equation (16). Electric field components are solved for "*In-plane vector*". This option is appropriated since there is no out-of-plane component of the electric field for the TM polarization.

Numeric Port boundary conditions are applied at the left and right boundaries. Wave excitation is "On" at the left side to lunch the guided wave, and "Off" at the right boundaries to avoid back-reflection of the propagating wave, so that guided wave is perfectly absorbed by the passive numerical port on the right side.

This model considers a section of a waveguide that is finite in the y direction. Because the fields drop off exponentially outside the waveguide, the fields can be assumed to be zero at some distance away from interfaces. This makes the boundary conditions in the y direction irrelevant, assuming that they are imposed sufficiently far away from interfaces.

Numerical Port boundary conditions require first solving an eigenvalue problem that solves for the fields and propagation constants at the boundaries. Study set up consists of two *Boundary Mode Analysis* steps followed by *Frequency Domain* step.

Global ODEs and DAEs (ge) interface is used to solve five transcendental algebraic equations (5), (6), and (12) in order to compare numeric and analytic solutions.

7. Results and Discussion

Field profiles in the DMD waveguide for the case of $k_0a=0.2$ are shown in . The fields extend into the dielectric and metal regions, but they are confined to distances that are less than their free-spaces wavelength. The longitudinal tangential component of the electric field E_x and transverse normal component of the magnetic field H_y are continuous across the interfaces, while longitudinal normal component of the electric field E_y is discontinuous. Results are in agreement with analytic solution shown in Figure 3 by dashed lines.

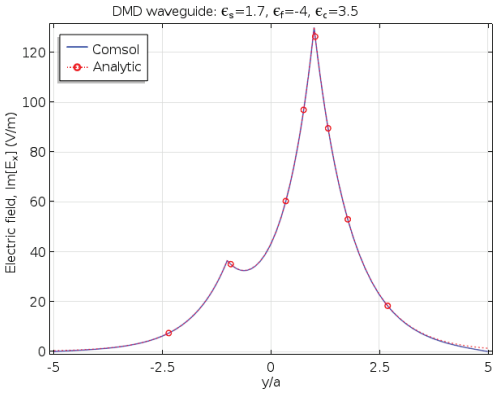

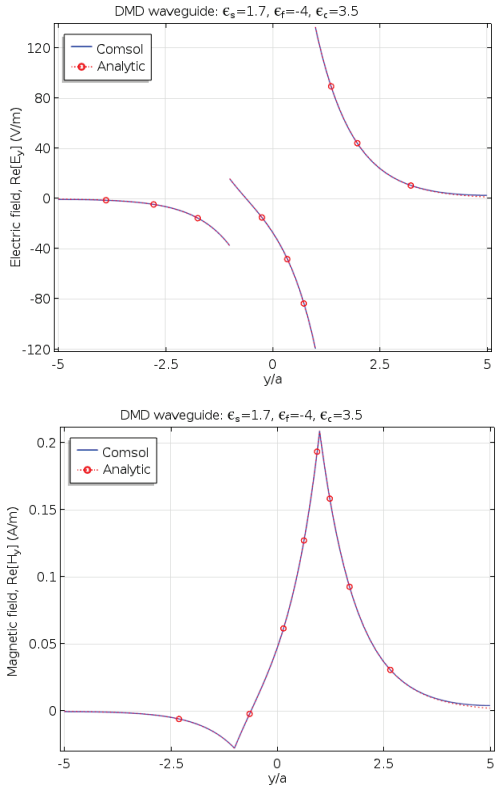

Figure 3. Field profiles in DMD waveguide, $k_0 a = 0.2$.

The dispersion curve is shown in Figure 4. Note that propagation constant is decreasing function of frequency. For the considered parameters of the DMD waveguide, TM mode propagates with no cutoff frequency. As the frequency increases, the magnetic field tends to be mode concentrated at the $\varepsilon_f - \varepsilon_c$ metal-dielectric interface, and solution tends to the single-interface solution as $\omega \to \infty$. Again, numerical results are in agreement with analytic solution shown in Figure 3 by dashed lines. Distributions of the electric field for the cases of $k_0 a = 0.1$ and $k_0 a = 0.7$ are shown in Figure 5.

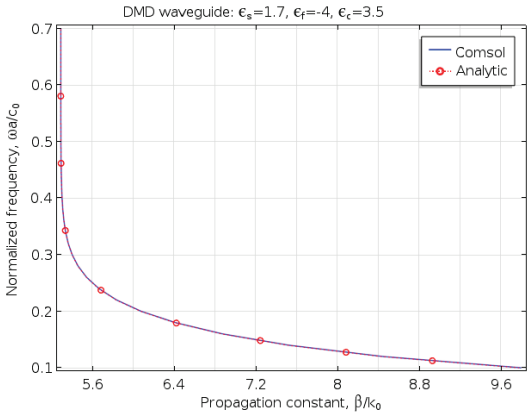

Figure 4. Dispersion curve for DMD waveguide

Results for the analysis of the MDM waveguide are shown in Figure 6 through Figure 7. Field profiles for the case $k_0 a = 0.6$ are shown in Figure 6. The dispersion curve appears in Figure 7. Unlike the DMD waveguide considered above, the propagation constant of the MDM waveguide is an increasing function of frequency. There is lower cutoff frequency, which can be calculates as [2]:

$$f_{cutoff} = \frac{c_0}{4\pi a}\left(\frac{|\varepsilon_c|}{\varepsilon_f + \sqrt{\varepsilon_f + |\varepsilon_c|}} + \frac{|\varepsilon_s|}{\varepsilon_f + \sqrt{\varepsilon_f + |\varepsilon_s|}}\right) \quad (17)$$

For the MDM waveguide parameters considered here, numerical value of the cutoff frequency is $f_{cutoff} = 51.7THz$ and cutoff value of the normalized wavenumber is $(ka)_{cutoff} = 0.542$. The upper limit for the propagation constant is defined by the following relation:

$$\beta \le \beta_\infty = k_0 \sqrt{\frac{\varepsilon_c \varepsilon_f}{\varepsilon_c + \varepsilon_f}} \quad (18)$$

The limit β_∞ is the wavenumber of a surface plasmon at the $\varepsilon_f - \varepsilon_c$ metal-dielectric interface as $\omega \to \infty$. Numerical value of the upper limit is $\beta_\infty = 2.211 k_0$. Field

distributions near the lower cutoff frequency and upper limit are shown in Figure 5.

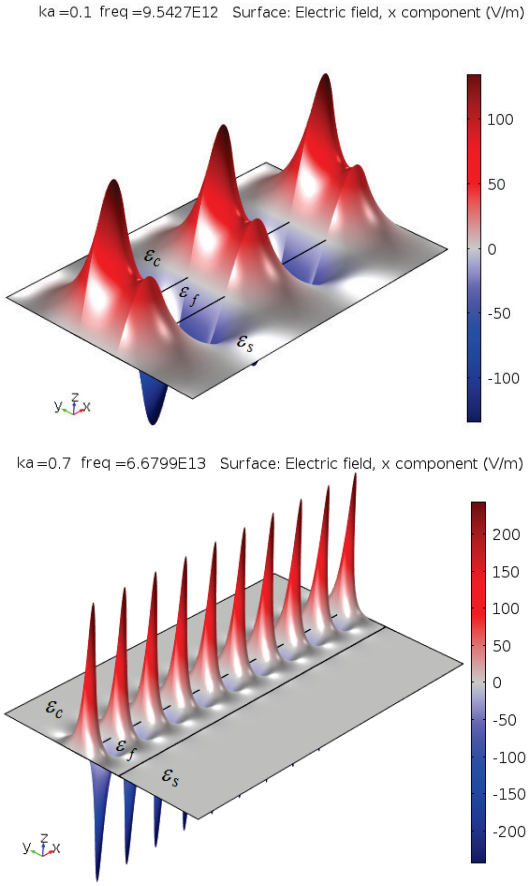

Figure 5. Electric field distribution in DMD waveguide at $ka = 0.1$ ($f = 9.54THz$, left) and $ka = 0.7$ ($f = 66.8THz$, right).

As an example of surface plasmonic wave propagation in a more complicated structure, consider a coplanar waveguide. Geometry of the basic surface plasmon coplanar waveguide (SP CPW) is shown in Figure 8. A dielectric substrate (D) has metal layers (M) of thickness t patterned on top of the substrate. A central metal layer of width w is separated by gap distance g from the side wide layers. The modeling methodology is outlined in the verification example of the layered plasmonic waveguide.

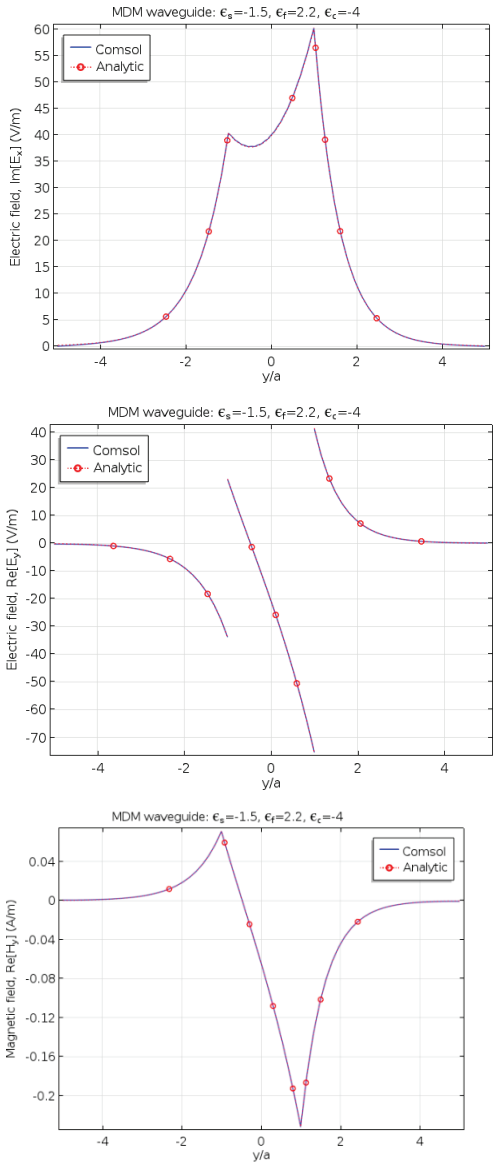

Figure 6. Field profiles in MDM waveguide, $k_0 a = 0.6$.

Geometry parameters of the analyzed waveguide are: $w = g = 50nm$, $h = 100nm$. Dielectric substrate is SiO_2 with dielectric constant $\varepsilon_{SiO_2} = 3.8$. Metal layers are silver. The Drude model dielectric function for Ag is [3]:

$$\varepsilon_{Ag}(\omega) = \varepsilon_\infty - \frac{\omega_p^2}{\omega(\omega - j\gamma_0)} \qquad (19)$$

where $\varepsilon_\infty = 3.7$, $\omega_p = 13.8 \cdot 10^{15}\, rad/s$, $\gamma_0 = 2.736 \cdot 10^{13}\, rad/s$, which is consistent with experimental data by Johnson and Christy [4]. Operating free-space wavelength is $\lambda_0 = 1500nm$.

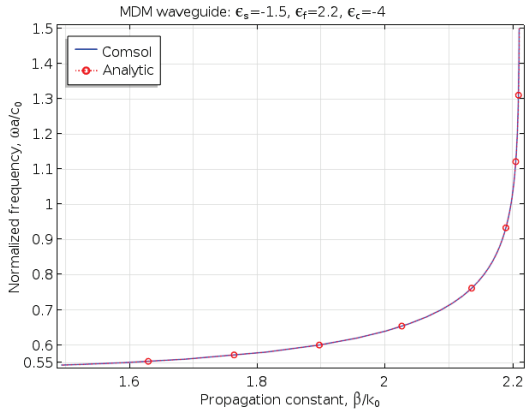

Figure 7. Dispersion curve for MDM waveguide.

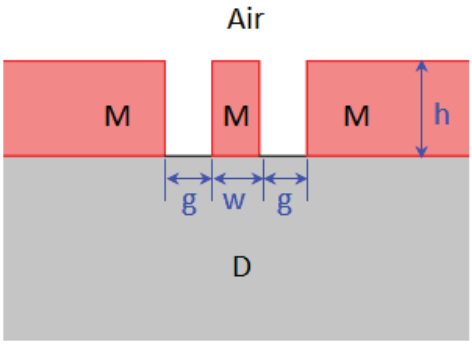

Figure 8. Geometry of surface plasmon coplanar waveguide.

There are two fundamental propagations modes with subwavelength confinement. Propagation constants of these modes are $\beta_1 / k_0 = 1.948 - j8.68 \cdot 10^{-3}$, and $\beta_2 / k_0 = 1.456 - j3.96 \cdot 10^{-3}$.

The first propagation constant corresponds to the even mode and the second represents the odd mode. Distribution of the longitudinal component of the electric field along the center line of the metal layers for even and odd modes is shown in Figure 9. Power of the propagating modes is well confined around the central metal strip, as shown in Figure 10.

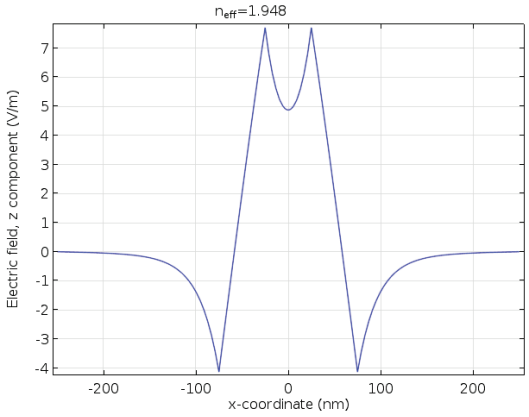

(a)

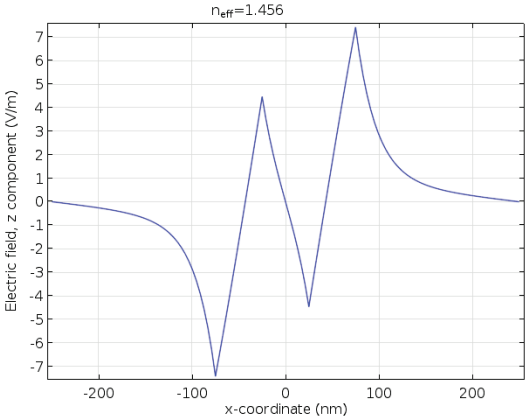

(b)

Figure 9. Distribution of the longitudinal electric field component along the center line of metal layers for SP CPW (a) even mode and SP CPW (b) odd mode .

8. Conclusions

Plasmonic layered waveguides in DMD and MDM configurations are considered and analyzed. Analytical solutions provide verification of the analysis methodology. This verified modeling technique is extended to the analysis of more complicated geometrical configuration of surface plasmon coplanar waveguide and subwavelength confinement of the propagating fundamental modes is illustrated.

9. References

1. D. Sarid and W. A. Challener, *Modern Introduction to Surface Plasmons, Theory,*

Mathematica Modeling and Applications, Cambridge University Press, Cambridge, 2010.

2. *Electromagnetic Waves and Antennas*, Sophocles J. Orfanidis, www.ece.rutgers.edu/~orfanidi/ewa/

3. C. Sönnnichsen, Plasmons in Metal Nanostructures, Ph. D., Ludwig-Maximilians-University of Munich, 2001.

4. P. B. Johnson and R. W. Christy, "Optical constants of the noble metals," *Phys. Rev. B*, vol. 6, no. 12, pp. 4370–4379, Dec. 1972.

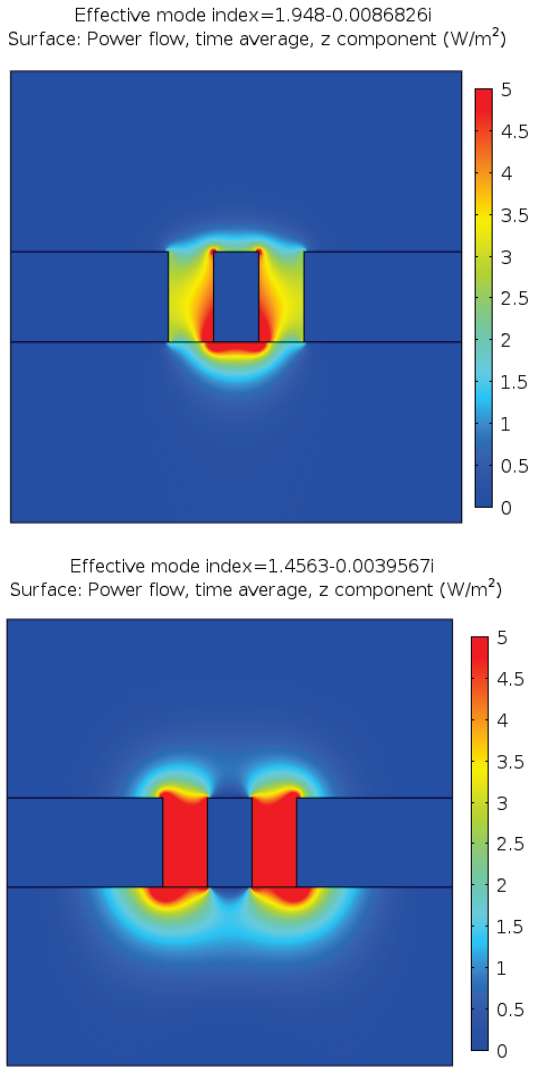

Figure 10. Power flow distribution for SP CPW even mode (left) and SP CPW odd mode (right).